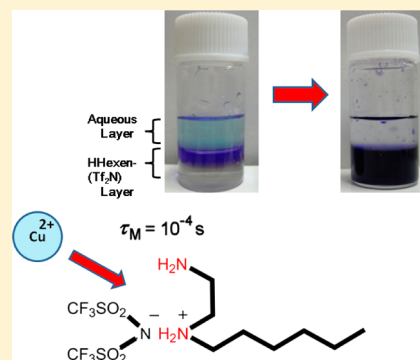


Solvation Structure of a Copper(II) Ion in Protic Ionic Liquids Comprising *N*-Hexylethylenediamine

Shinobu Takemura,[†] Sayaka Kawakami,[†] Masafumi Harada,[‡] and Masayasu Iida^{*,†}[†]Department of Chemistry, Faculty of Science, and [‡]Department of Textile and Apparel Science, Faculty of Human Life and Environmental Sciences, Nara Women's University, Kita-uoya-nishi-machi, Nara 630-8506, Japan

Supporting Information

ABSTRACT: The fine and dynamic structure of the copper(II) ion solvated in a protic ionic liquid (PIL) comprising monoprotonated *N*-hexylethylenediaminium (HHexen⁺) and bis(trifluoromethanesulfonyl)amide (Tf₂N⁻) [or trifluoroacetate (TFA⁻)] was determined using NMR, visible electronic, and extended X-ray absorption fine structure (EXAFS) spectroscopy. The chelate-diamine group in the cationic unit facilitates advantageous dissolution of transition-metal salts in the present PIL. The interaction of the copper(II) ion with the chelate-diamine PIL was explored by the addition of copper(II) salts to the PIL, demonstrating competitive complexation between the ligand of the added copper(II) salt and the components of the ionic liquid to the copper(II) ion. The favorable mode of interaction of the present chelating PIL with the copper(II) ion was clarified based on a comparison of the interactions with analogous liquids, including the monoprotonated hexylammonium HHexam(Tf₂N)-PIL, neat *N*-hexylethylenediamine (Hexen), and neat ethylenediamine (En). The coordination modes of the bis-Hexen and tris-Hexen copper(II) complexes in molecular liquids and in solids were also studied for comparison of the coordination structures around the copper(II) ion with those in the present PILs. The paramagnetic-induced relaxations derived from ¹³C (ΔT_{1p}^{-1}) and ¹⁵N (ΔT_{2p}^{-1}) NMR, the visible electronic spectra, and EXAFS analysis showed that the copper(II) ion tends to form a bis-Hexen complex in the HHexen-PIL despite the electrostatic repulsion and the fact that the counteranions are located at the axial sites, whereas in the HHexam(Tf₂N)-PIL, the copper(II) ion exhibits affinity for the Tf₂N anion over the protonated amines. The lifetime of the copper(II) complex formed in the PIL was determined to be $\approx 10^{-4}$ s based on ¹³C (ΔT_{1p}^{-1}) and ¹⁴N (ΔT_{2p}^{-1}) NMR, which is appreciably longer than that in conventional molecular solvents.



INTRODUCTION

The fascinating properties of room temperature ionic liquids (RTILs) for nanoscale reactions are derived from their novel nanostructures comprising hydrophilic–hydrophobic mixing domains.¹ Owing to their peculiar structure, RTILs have successfully been used as templates for the synthesis of inorganic nanomaterials having novel morphologies or improved properties.² Ionic liquids of transition-metal complexes (metILs) are particularly interesting as functional inorganic–organic hybrid soft-materials.³ Certain RTILs have been utilized in solvent extraction processes based on their enhanced distribution coefficients in the extraction of metal ions from aqueous solutions.⁴ These functional advantages of ILs may be derived from their moderate hydrophilic–hydrophobic balance as well as their nanostructures that bear similarity to microemulsions.

It is, however, generally difficult to dissolve transition-metal salts in conventional aprotic ionic liquids without chelating agents. In most cases, when metal ions are adequately (more than 0.1 mol kg⁻¹) dissolved in ionic liquids, they are encapsulated in the anionic unit to form anionic metal complexes.⁵ For widespread application of IL systems in the

fields of electrochemistry and analytical chemistry, it is necessary for ILs to universally dissolve metal salts.

The incorporation of a larger hydrophilic region in the ion-pairing structure seems to be an important parameter for more extensive concentration of metal ions in the IL systems.⁶ From this point of view, protic ionic liquids (PILs)⁷ with chelating rings are prospective candidates that may universally accept transition-metal ions. In our previous studies, a series of PILs based on the alkylethylenediaminium cation⁸ was isolated and the physical properties of the PILs were evaluated. ¹⁵N NMR chemical shift analysis revealed that the ionicities of the two PILs comprising HHexen(X) [HHexen = monoprotonated hexylethylenediamine; X = bis(trifluoromethanesulfonyl)amide (Tf₂N); in previous papers abbreviated as “TFSA”) or trifluoroacetate (TFA)] were similar.^{8c}

On the basis of this previous study, we herein focus on the unique solvation structure of copper(II) ions in this novel HHexen(Tf₂N) solvent, where the metal ions are encapsulated in the limited ion-pairing region. In the study of ILs as “the third solvent”, it is fundamental to specify the mode of

Received: May 20, 2014

Published: September 4, 2014

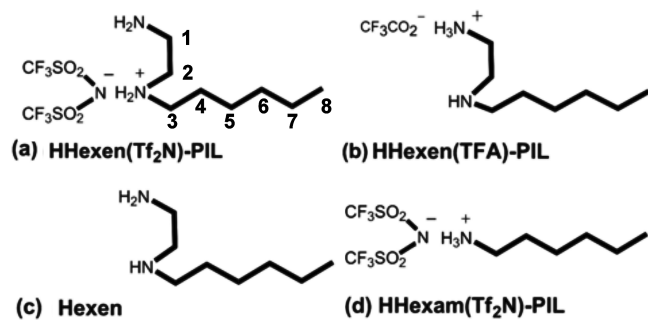


interaction of the ILs with metal ions, i.e., the solvation structure of the metal ions in the ILs. However, there is a dearth of information regarding these solvation structures, and the majority of prior studies have concentrated on anionic metal complexes.⁹ The present PIL system facilitates the systematic evaluation of the specific interaction of the PILs with Cu^{2+} in comparison with analogous systems. On the basis of electrostatic interactions, metal ions exhibit a higher affinity for the anionic unit of ILs over the cationic unit, whereas it is plausible that the En headgroup may accept metal ions because of the chelating effect. The mode of interaction of the chelating PILs with copper(II) ions is elucidated herein based on a comparison with analogous liquids. In the present unique complexation system, the mode of coordination of the copper(II) ion in the PILs is specified using ^{13}C , ^{15}N , and ^{14}N NMR, extended X-ray absorption fine structure (EXAFS) for the copper(II) ion, and visible electronic spectroscopy.

EXPERIMENTAL SECTION

Materials. *N*-Hexylethylenediamine [abbreviated as Hexen or hexen (in the copper(II) complexes)] was prepared by the reaction between 1-bromohexane and ethylenediamine (1:5 molar ratio) according to the literature.¹⁰ The Hexen liquid obtained by distillation contained a small amount of water (800 ppm, i.e., $W_0 = 6.5 \times 10^{-3}$, where W_0 is defined as $[\text{H}_2\text{O}]/[\text{Hexen}]$ and was determined by a Karl Fischer titration), which was reduced to 60 ppm ($W_0 = 5 \times 10^{-4}$) by passing the liquid over molecular sieves (3A 1/16; Wako Chemicals). Herein, the two forms of neat Hexen are distinguished by denoting the former as wet-Hexen and the latter as dry-Hexen; dry-Hexen was used in most cases for comparative analysis of the PILs, unless otherwise stated. Ethylenediamine [abbreviated as En or en (in the copper(II) complexes)] of guaranteed reagent (G.R.) grade supplied by Wako Chemicals was used after single distillation, where the water content was 1750 ppm ($W_0 = 6 \times 10^{-3}$). Chloroform (ClF) of G.R. grade, supplied by Wako Chemicals, was purified by a previous procedure to remove the small amount of ethanol (EtOH),¹¹ and its final water content was 2.5 ppm ($W_0 = 1.5 \times 10^{-4}$). EtOH was singly distilled prior to use, and the water content was 17300 ppm ($W_0 = 4.5 \times 10^{-2}$). The PILs used were monoprotonated *N*-hexylethylenediaminium (HHexen⁺) or hexylammonium salts with the Tf_2N (or TFA) counteranion, i.e., respectively abbreviated as HHexen(Tf_2N), HHexen(TFA), and HHexam(Tf_2N) hereafter (Scheme 1). The

Scheme 1. HHexen⁺-PILs (a and b) and Analogous Liquids Such as (c) Hexen and (d) HHexam(Tf_2N)-PIL



PILs were prepared by neutralization [mixing of 1.0 (base):1.0 (acid) molar ratio] of the original amines (Hexen was prepared as described above and Hexam was supplied by Tokyo Kasei Chemicals) with HTf_2N (Tf_2N acid, supplied by Morita Chemicals) or HTFA (TFA acid, supplied by Wako Pure Chemicals) in diethyl ether solution and then isolated by a complete evaporation of the diethyl ether. The characterization and physical properties of the HHexen(Tf_2N) and HHexen(TFA) salts have been reported in detail in a previous

paper.^{8b,c} The purity of the products was confirmed based on the ^{13}C NMR and CHN elemental analyses. The water content (W_0) was ca. 6×10^{-4} (25 ppm) for the HHexen(Tf_2N)-PIL, 0.015 (1000 ppm) for the HHexen(TFA)-PIL, and 6×10^{-4} (30 ppm) for the HHexam(Tf_2N)-PIL.

The pH neutrality of all of the prepared PILs was checked by pH measurement (Horiba D-51 pH meter) of the aqueous layer of the water/PIL double layer (5:1, v/v) for the HHexen(Tf_2N)- and HHexam(Tf_2N)-PILs or a 0.1 mol kg^{-1} aqueous solution in the case of HHexen(TFA) [see SI-1 in the Supporting Information (SI)].

Notably, a previous study by the current research group demonstrated that when the copper(II) ion is encapsulated in the HHexen-PILs, the protons are released from the ethylenediaminium cation, whereas the change in the pH of the PILs accompanying the deprotonation is suppressed by the buffer action of the En headgroup.^{8c}

The purity of the PILs was confirmed using CHN elemental analyses (SI-1 in the SI) and ^{13}C and ^{15}N NMR spectroscopy. Hexyltrimethylammonium bromide (HTMAB) used for the titration analysis of λ_{max} of $\text{Cu}(\text{hexen})_2(\text{Tf}_2\text{N})_2$ in ClF was of G.R. grade from Tokyo Chemical Industries. The copper(II) salts used as additives to the PILs were supplied as follows. $\text{CuCl}_2 \cdot 2\text{H}_2\text{O}$ (G.R.) and CuBr_2 (99.9%) were from Wako Pure Chemicals, and $\text{Cu}(\text{NH}_3)_4(\text{NO}_3)_2$ (99%) was from Mitsuwa Chemicals. $\text{Cu}(\text{Tf}_2\text{N})_2$ [or $\text{Cu}(\text{TFA})_2$] was prepared by the reaction of $\text{Cu}(\text{OH})_2$ with HTf_2N (or HTFA; 1:2 molar ratio) in a methanol solution. After removing the residual $\text{Cu}(\text{OH})_2$, we condensed the solution in a rotary evaporator until a small amount of the light-blue crystal precipitated. The solution was left to stand in a refrigerator, and the light-blue products obtained were collected and then dried under vacuum for several days. Furthermore, $[\text{Cu}(\text{hexen})_2]\text{X}_2$ ($\text{X} = \text{Br}, \text{Tf}_2\text{N}, \text{and TFA}$) was prepared for the acquisition of the visible electronic spectra and EXAFS measurements as follows. A total of 2 mol equiv of Hexen was added to an aqueous solution of CuX_2 salt, and then the solution was condensed in a rotary evaporator until a small amount of the purple-blue crystal precipitated ($[\text{Cu}(\text{hexen})_2](\text{Tf}_2\text{N})_2$ and $[\text{Cu}(\text{hexen})_2]\text{Br}_2$ readily precipitated from the aqueous solution). The $[\text{Cu}(\text{hexen})_2]\text{X}_2$ complexes were newly synthesized in this work, and the results of CHN elemental analyses are written in SI-1 in the SI.

NMR Measurements. The longitudinal relaxation times (T_1) were obtained for the ^{13}C NMR spectra, and the line widths ($\Delta\nu_{1/2} = 1/\pi T_2$, where T_2 is the transverse relaxation time) were obtained for the ^{14}N and ^{15}N NMR spectra. The ^{13}C and ^{14}N NMR spectra were respectively recorded at 67.9 and 19.4 MHz on a JEOL EX-270 Fourier transform (FT) NMR spectrometer. The delay time was set to 100 μs for the ^{14}N NMR measurement. On the basis of the solubility data of the copper(II) salts in various solvents (Table 1), we prepared the sample solutions for the measurements of absorption spectra, NMR, and EXAFS using a 5 mL sample tube with a screw-on lid that closes tightly. The copper(II) salts were dissolved in 1–3 g solvent scales at the time that is as close as possible to each measurement. Therefore, there is little space for the samples contaminated by moisture.

The sample solution in the absence of the copper(II) ion was bubbled with argon gas for about 5 min just before each NMR measurement in order to remove any oxygen gas from the solution. The ^{13}C NMR longitudinal relaxation times (T_1) were measured by an inversion–recovery method, using the pulse sequence of (-180° pulse– t – 90° pulse– T –). For measurements of T_1 , 10 different pulse intervals (t) were used with a waiting time (T) of more than $10T_1$. The temperature dependence of the relaxation times (^{13}C) or line widths (^{14}N) was monitored by varying the temperatures in the range of 15–70 $^\circ\text{C}$ for acquisition of the ^{13}C NMR data, 20–70 $^\circ\text{C}$ for the ^{14}N NMR of Hexen, and 85–120 $^\circ\text{C}$ for the ^{14}N NMR of HHexen(Tf_2N). The ^{15}N NMR spectra in solution were recorded on a JEOL JNM Lambda-500 FT NMR spectrometer at 50.7 MHz in proton-decoupling bilevel complete decoupling mode. The NMR measurements were performed at 27 $^\circ\text{C}$ unless otherwise stated.

EXAFS Measurements. EXAFS measurements at the Cu K-edge (8980.3 eV) were performed at room temperature in transmission

Table 1. Solubility (mol kg⁻¹) of Some Copper(II) Salts in the PILs and Analogous Molecular Solvents^a

solvent	CuCl ₂ ·2H ₂ O	CuBr ₂	[Cu(NH ₃) ₄](NO ₃) ₂	Cu(Tf ₂ N) ₂	Cu(TFA) ₂
En	0.01	0.01	>0.3 ^b	>0.3	>0.3
wet-Hexen	0.02	0.20	0.25	>0.3	>0.3
dry-Hexen	<0.01 ^c	0.03	0.04	>0.3	>0.3
HHexen(Tf ₂ N)-PIL	0.20	0.20	0.20	0.10	<i>d</i>
HHexen(TFA)-PIL	0.15	0.15	0.20	<i>d</i>	0.15
HHexam(Tf ₂ N)-PIL	<0.01	<0.01	0.03	0.10	<i>d</i>

^aThe values between 0.10 and 0.25 mol kg⁻¹ have associated errors of ±0.03 mol kg⁻¹. ^b>*x*: more than *x*. ^c<*x*: less than *x* ^dThese systems were not examined.

mode at the BL-9C station of the Photon Factory, High Energy Accelerator Research Organization in Japan (KEK-PF). The experimental and analytical procedures were almost the same as those reported in a previous paper.¹² In the fitting of $k^3\chi(k)$, least-squares refinements of parameters R_p , N_p , and σ_i were performed to minimize the *r* factor (%). As references, the [Cu(NH₃)₄](NO₃)₂^{13a} crystal, [Cu(en)₃]SO₄ crystal,^{13b,c} [Cu(en)₂](NO₃)₂ crystal, 0.05 mol kg⁻¹ [Cu(en)₃]SO₄ aqueous solution ([Cu(en)₂(H₂O)₂]²⁺ in solution),¹⁴ and 0.05 mol kg⁻¹ [Cu(en)₃](TfO)₂ En solution ([Cu(en)₃]²⁺ in solution)¹⁴ were used to evaluate the validity of the theoretical phase shift and back-scattering amplitude functions proposed by McKale et al.¹⁵

Electronic Spectral Measurements. UV–visible–near-IR electronic spectra of the PILs containing copper(II) ions were acquired in the wavelength range of 400–1200 nm at intervals of 0.2 nm using a Jasco V-670iRM (single-beam) instrument at ambient temperature. The precision of the wavelength was ±0.3 nm. The cell length was 0.2, 0.1, or 1.0 cm. The spectra of the PILs themselves gave small and shoulder spectra in the visible region. (The absorbances were less than 0.1 and 0.005 at 400 and 500 nm, respectively; ϵ_{\max} at $\lambda_{\max} = 337.5$ nm is 4.2 kg mol⁻¹ cm⁻¹.) The background spectrum of the solvent was subtracted from all of the copper(II) spectra. The procedure for the preparation of the sample solutions was described in the NMR section.

Other Measurements. The kinematic viscosities (ν) of Hexen and HHexen(Tf₂N) in the presence and absence of Cu²⁺ were measured with a Cannon–Fenske capillary viscometer at 27 °C. The shear viscosity (η) was obtained from the relationship $\eta = \nu\rho$, where the density (ρ) was measured by using an Ostwald-type picnometer. After extraction of CuSO₄ from a 0.05 mol kg⁻¹ aqueous solution by the HHexen(Tf₂N)-PIL, the copper(II) ion concentration in the aqueous layer was measured using a copper-ion meter (JAPAN-ION Corp.).

RESULTS AND DISCUSSION

Solubility of Copper(II) Salts in the HHexen-PILs and Analogous Liquids. The copper(II) salts CuCl₂·2H₂O, CuBr₂, [Cu(NH₃)₄](NO₃)₂, Cu(Tf₂N)₂, and Cu(TFA)₂ were used as additives for analysis of the interaction of the copper(II) ion with HHexen(Tf₂N)-PIL [or HHexen(TFA)-PIL], where the protonation sites of the two HHexen-PILs were determined in the previous study^{8c} in comparison with the analogous liquids HHexam(Tf₂N)-PIL, neat Hexen, and neat En (Scheme 1, except for En). The solubility was estimated based on attempts to dissolve the copper(II) salts in each solvent at 30 °C over 3 weeks. Although dissolution of the salts in the PILs generally required time to attain equilibrium and thus the solubility data listed in Table 1 are somewhat rough, the following significant trends were observed: (1) Simple copper(II) salts such as CuCl₂·2H₂O and CuBr₂ are dissolved more readily in wet-Hexen than in En with a similar water content [$W_0 \approx (6-6.5) \times 10^{-3}$], whereas these copper salts were much less soluble in dry-Hexen ($W_0 \approx 5 \times 10^{-4}$). This property suggests the formation of an organized structure of Hexen like a reverse micelle, in which the metal salts are

effectively collected in the headgroup region.^{6,16} (2) All of the copper(II) salts dissolved significantly in the HHexen(Tf₂N)-PIL ($W_0 \approx 6 \times 10^{-4}$) and HHexen(TFA)-PIL ($W_0 \approx 0.015$). It is remarkable that CuCl₂·2H₂O dissolved to a greater extent in the HHexen(Tf₂N)-PIL ($W_0 \approx 6 \times 10^{-4}$) than in wet-Hexen ($W_0 \approx 6.5 \times 10^{-3}$) and that CuCl₂·2H₂O and CuBr₂ are much less soluble in dry-Hexen than in the HHexen(Tf₂N)-PIL with a similar water content [$W_0 \approx (5-6) \times 10^{-4}$]. These results clearly indicate the appreciably higher solubility of the copper(II) salts in the HHexen(Tf₂N)-PIL compared to Hexen having a similar water content [the lower solubility of Cu(Tf₂N)₂ in HHexen(Tf₂N) and Cu(TFA)₂ in HHexen(TFA) is due to the common ion (anion) effect]. (3) The simple copper(II) salts are not readily dissolved in the monoamine HHexam(Tf₂N)-PIL ($W_0 \approx 5 \times 10^{-4}$), whereas Cu(Tf₂N)₂ is relatively soluble in this PIL because Cu²⁺ will be incorporated into the counteranionic unit of the PIL as described below. The remarkable solubilities of the copper(II) salts in the HHexen-PILs can be attributed to the cooperative effect of the chelate ring in the cationic unit with the ion-pairing structure.

An advantage of the HHexen(Tf₂N)-PIL as a solvent compared to other analogous liquids was observed in the extraction of the copper(II) ion from aqueous solution. Although wet-Hexen and the HHexen(TFA)-PIL also dissolve in copper(II) salts, these liquids are sufficiently hydrophilic to be miscible with water. Furthermore, HHexam(Tf₂N)-PIL is too hydrophobic to extract aqueous copper(II) ion probably because of the absence of the chelate ring in the Hexam molecule. Thus, these liquids are unavailable for the extraction of copper(II) ion from water. In contrast, the HHexen(Tf₂N)-PIL not only dissolves copper(II) salts extensively but is also almost immiscible with water (less than 0.1 wt %). If a 0.05 mol kg⁻¹ CuSO₄ aqueous solution was combined with an equivalent volume of HHexen(Tf₂N), the concentration of copper(II) ions in the upper layer of the aqueous solution would decrease to a final concentration of ca. 3 ppm (4.6×10^{-5} mol kg⁻¹); that is, ca. 99.9% of the copper(II) ion would move from the aqueous layer to the PIL layer.

Visible Electronic Spectra of Copper(II) Ions in Molecular Solvents. Before the electronic spectra of the copper(II) ion in the PIL systems is discussed, the spectra of the en and hexen copper(II) complexes in molecular solvents should first be elucidated. The assignment of the spectra for successive complexation (i.e., the bis-en and tris-en complexes) of Cu²⁺ with the en ligands in water or in neat En has been well established, and the profiles of the spectra of the bis-en and tris-en complexes in solution were confirmed herein^{14,17} (SI-2 and Figure S1 in the SI). Because the monodentate ligands in the axial sites of the copper(II) complexes with two chelating ligands are more easily displaced by the solvents due to the

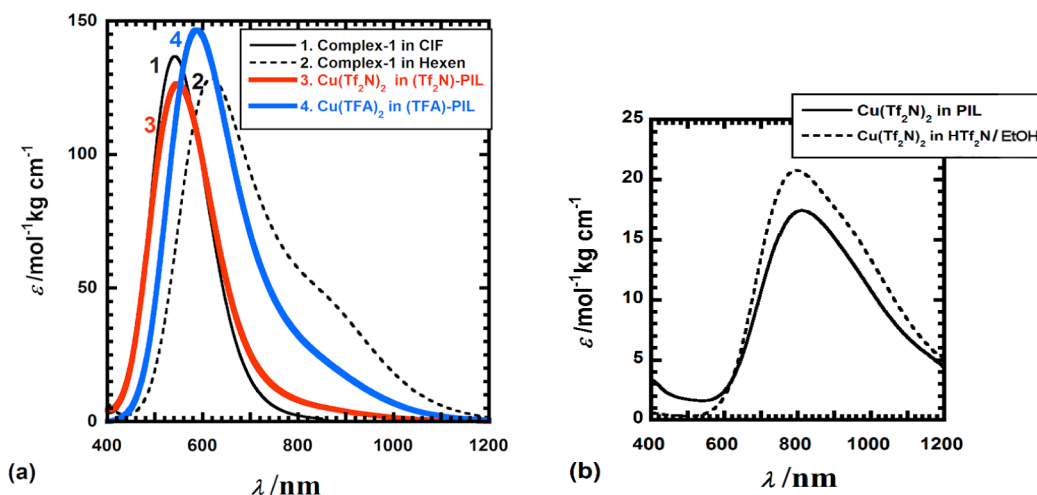


Figure 1. Electronic absorption spectra: (a) 1, $[\text{Cu}(\text{hexen})_2](\text{Tf}_2\text{N})_2$ (Complex-1) in ClF, where $[\text{Cu}(\text{hexen})_2]^{2+}$ is major in solution; 2, $[\text{Cu}(\text{hexen})_2](\text{Tf}_2\text{N})_2$ in Hexen, where $[\text{Cu}(\text{hexen})_3]^{2+}$ is major in solution; 3, $\text{Cu}(\text{Tf}_2\text{N})_2$ in HHexen(Tf_2N)-PIL; 4, $\text{Cu}(\text{TFA})_2$ in HHexen(TFA)-PIL. (b) solid line, $\text{Cu}(\text{Tf}_2\text{N})_2$ in HHexam(Tf_2N)-PIL; broken line, $\text{Cu}(\text{Tf}_2\text{N})_2$ in a $\text{HTf}_2\text{N}/\text{EtOH}$ concentrated solution (20.9 mol kg^{-1}).

Jahn–Teller effect than the chelating equatorial ligands, the wavelength of maximum absorbance (λ_{max}) of this type of complex is sometimes useful for monitoring the donor numbers of the solvents.^{18,19}

Information regarding the coordination structures of the en complexes in solution can be simply extended to the hexen complexation systems. The visible electronic spectra of $[\text{Cu}(\text{hexen})_2]\text{X}_2$ in ClF, where the donor number is small (≈ 4),^{19b} were acquired (Figure 1a, solid line 1), and the λ_{max} data are presented in Table 2(I). The data can be interpreted as

Table 2. $\lambda_{\text{max}}/\text{nm}$ Values of (I) $[\text{Cu}(\text{hexen})_2]\text{X}_2$ in ClF, EtOH, and Hexen (for $\text{X} = \text{Tf}_2\text{N}^-$ in ClF at $0.001\text{--}0.01 \text{ mol kg}^{-1}$; for the Other Systems at $0.01\text{--}0.10 \text{ mol kg}^{-1}$) and (II) Limiting for Cu^{2+} in the PILs

(I)				
solvent	$\lambda_{\text{max}}/\text{nm}$ for $[\text{Cu}(\text{hexen})_2]\text{X}_2$, where $\text{X} =$			
	Tf_2N		TFA	Br
ClF	542	<	599	< 613
EtOH	560	<	575	< 588
Hexen	618		590 ^a	610 ^a
(II)				
PIL	limiting $\lambda_{\text{max}}/\text{nm}$ for Cu^{2+} (Figure 2)			
HHexen(TFA)	590			
HHexen(Tf_2N)	550			
HHexam(Tf_2N)	(780) ^b			

^aBelow 0.01 mol kg^{-1} , these values increase with a decrease in the concentration to approach 618 nm ^bCoordinated mainly by Tf_2N .

follows. The order of the λ_{max} values in ClF can be explained on the basis of the donor numbers $[\text{Tf}_2\text{N}^- (\approx 4) < \text{TFA}^- < \text{Br}^-]$ ^{18–20} of the counteranions (X) of $[\text{Cu}(\text{hexen})_2]\text{X}_2$ because in ClF the X anion may coordinate primarily to Cu^{2+} . On the other hand, the order of the λ_{max} values in EtOH and Hexen indicates a partial or full replacement of the counteranions in the axial positions by the solvent based on the order of the donor numbers: $\text{ClF} \approx \text{Tf}_2\text{N}^- < \text{EtOH} < \text{TFA}^- < \text{Br}^- < \text{Hexen}$. The medium λ_{max} value for each X salt is achieved in EtOH because of the medium donor number of EtOH, whereas the order still follows the strength of the basicity of X.

In Hexen, the λ_{max} value of the $[\text{Cu}(\text{hexen})_2](\text{Tf}_2\text{N})_2$ complex is almost constant over the wide concentration range of the copper(II) salts (Table 2(I) and Figure 2, system

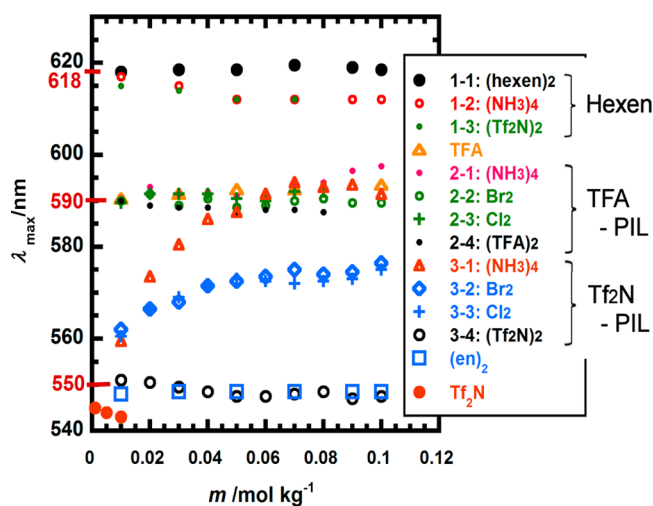


Figure 2. λ_{max} values of the copper(II) ion in various solvents as a function of the added copper(II) salt concentrations. The legends are as follows: 1-1, $[\text{Cu}(\text{hexen})_2](\text{Tf}_2\text{N})_2$ in Hexen ($[\text{Cu}(\text{hexen})_2]^{2+}$ in solution); 1-2, $[\text{Cu}(\text{NH}_3)_4](\text{NO}_3)_2$ in wet-Hexen; 1-3, $\text{Cu}(\text{Tf}_2\text{N})_2$ in Hexen; TFA, $[\text{Cu}(\text{hexen})_2](\text{TFA})_2$ in ClF; 2-1, $[\text{Cu}(\text{NH}_3)_4](\text{NO}_3)_2$ in HHexen(TFA)-PIL; 2-2, CuBr_2 in HHexen(TFA)-PIL; 2-3, $\text{CuCl}_2 \cdot 2\text{H}_2\text{O}$ in HHexen(TFA)-PIL; 2-4, $\text{Cu}(\text{TFA})_2$ in HHexen(TFA)-PIL; 3-1, $[\text{Cu}(\text{NH}_3)_4](\text{NO}_3)_2$ in HHexen(Tf_2N)-PIL; 3-2, CuBr_2 in HHexen(Tf_2N)-PIL; 3-3, $\text{CuCl}_2 \cdot 2\text{H}_2\text{O}$ in HHexen(Tf_2N)-PIL; 3-4, $\text{Cu}(\text{Tf}_2\text{N})_2$ in HHexen(Tf_2N)-PIL; (en)₂, $[\text{Cu}(\text{en})_3]\text{SO}_4$ in water ($[\text{Cu}(\text{en})_2(\text{H}_2\text{O})_2]^{2+}$ in solution); Tf_2N , $[\text{Cu}(\text{hexen})_2](\text{Tf}_2\text{N})_2$ in ClF ($[\text{Cu}(\text{hexen})_2]^{2+}$ in solution).

1-1), which indicates that the ligands of the added copper(II) salts are easily replaced by the hexen ligand in the neat Hexen liquid and the tris-Hexen complex is primarily formed.

The distorted shape of the spectrum of this system (Figure 1a, line 2) similar to that of $[\text{Cu}(\text{en})_3]^{2+}$ (Figure S1, broken line, in the SI) supports this view as well. The same trend is nearly seen for $[\text{Cu}(\text{NH}_3)_4](\text{NO}_3)_2$ and $\text{Cu}(\text{Tf}_2\text{N})_2$ in Hexen (Figure 2, systems 1-2 and 1-3). For the $\text{X} = \text{Br}$ and TFA

complexes of $[\text{Cu}(\text{hexen})_2]\text{X}_2$, the tris-Hexen complex may be formed at copper(II) concentrations below 0.01 mol kg^{-1} , as presented in Table 2(I).

Visible Electronic Spectra of Copper(II) Ions in the PILs. The λ_{max} values of the copper(II) ions in the visible electronic spectra of the two HHexen-PILs were found to be dependent on the copper(II) salt concentration to some extent, as shown in Figure 2, which presents λ_{max} of $[\text{Cu}(\text{NH}_3)_4(\text{NO}_3)_2]$ and $\text{Cu}(\text{Tf}_2\text{N})_2$ in Hexen (systems 1-2 and 1-3, respectively), $[\text{Cu}(\text{hexen})_2](\text{Tf}_2\text{N})_2$ and $[\text{Cu}(\text{hexen})_2](\text{TFA})_2$ in ClF (denoted as “ Tf_2N ” and “ TFA ”, respectively, in the legend), and $[\text{Cu}(\text{en})_3]\text{SO}_4$ in an aqueous solution ($[\text{Cu}(\text{en})_2(\text{H}_2\text{O})_2]^{2+}$; denoted as “ $(\text{en})_2$ ” in the legend) for comparison. Typical spectra of copper(II) in the PILs are presented in Figure 1a. Figure 2 shows that, at the limiting zero concentration of copper(II), the λ_{max} value of copper(II) in the HHexen(Tf_2N)-PIL generally approaches 550 nm (systems 3-1–3-4), whereas in the HHexen(TFA)-PIL, the value generally approaches 590 nm (systems 2-1–2-4). In the HHexen(A)-PIL system (A = Tf_2N or TFA), it is notable that the λ_{max} value at the limiting zero concentration is close to that of $[\text{Cu}(\text{hexen})_2](\text{A})_2$ rather than that of $[\text{Cu}(\text{hexen})_3]^{2+}$. These results indicate that, at the limiting zero concentration of copper(II) in the HHexen(A)-PIL, the mode of coordination around the copper(II) ion approximates those of the $[\text{Cu}(\text{hexen})_2](\text{A})_2$ complex in ClF, where the two Hexen ligands coordinate at the equatorial position and the A anion coordinates at the axial position. In the HHexen(Tf_2N)-PIL system, as the concentration of the copper(II) salt increases, the two Tf_2N anions at the axial positions are gradually replaced by the ligands of the added copper(II) salts, whereas the two Hexen ligands remain coordinated to copper(II). At a copper(II) salt concentration of 0.1 mol kg^{-1} , the order of λ_{max} follows the basicity (or donor number) order of the ligands: $\text{Tf}_2\text{N}^- < \text{Br}^- \approx \text{Cl}^- < \text{NH}_3 \approx \text{Hexen}$.

In order to further confirm the mode of coordination around the copper(II) ion in the PILs, the λ_{max} values of Cu^{2+} in the PILs were compared with that of $[\text{Cu}(\text{hexen})_2](\text{Tf}_2\text{N})_2$ during complexation with Br^- ions derived from HTMAB in ClF. The addition of HTMAB induced a sharp red shift of λ_{max} in the case of 0.01 mol kg^{-1} $[\text{Cu}(\text{hexen})_2](\text{Tf}_2\text{N})_2$ (Figure S2 in the SI); this change indicates a replacement of coordinated Tf_2N by Br^- . The λ_{max} value of $[\text{Cu}(\text{hexen})_2]\text{Br}_2$ in ClF is 613 nm [Table 2(I)], and Figure S2 in the SI suggests that if the two Tf_2N anions are completely replaced by the bromide ion in the axial position of $[\text{Cu}(\text{hexen})_2]^{2+}$ in ClF solution, the λ_{max} value becomes 613 nm. At a concentration of 0.1 mol kg^{-1} CuBr_2 , λ_{max} is 575 nm in the HHexen(Tf_2N)-PIL, as described in Figure 2, system 3-2. On the other hand, Figure S2 in the SI shows that the λ_{max} value is 575 nm when the $[\text{Br}^-]/[\text{Cu}(\text{hexen})_2]^{2+}$ ratio is around 0.3–0.4. These relationships between the replacement ratio of Tf_2N^- by Br^- in the axial position of $[\text{Cu}(\text{hexen})_2]^{2+}$ and the λ_{max} value indicate that, at a CuBr_2 concentration of 0.1 mol kg^{-1} in the Tf_2N -PIL (Figure 2, system 3-2), 15–20% of the two Tf_2N ligands at the axial position may be replaced by Br^- . When either $[\text{Cu}(\text{NH}_3)_4](\text{NO}_3)_2$ or $\text{CuCl}_2 \cdot 2\text{H}_2\text{O}$ is added to the HHexen(Tf_2N)-PIL, a similar phenomenon might occur (systems 3-1 and 3-3).

In the HHexen(TFA)-PIL system, on the other hand, replacement of the coordinating counteranions by the ligands of the added copper(II) salts does not occur to a significant extent (Figure 2, systems 2-1–2-4). These contrasting results for the Tf_2N and TFA anions are attributed to the larger

coordination strength (or donor number) of TFA compared to that of Tf_2N .

The addition of $\text{Cu}(\text{Tf}_2\text{N})_2$ to the HHexen(Tf_2N)-PIL and of $\text{Cu}(\text{TFA})_2$ to the HHexen(TFA)-PIL produce no significant change in the λ_{max} value, and thus the copper(II) coordination in these systems remains largely unchanged upon the addition of the copper(II) salts to the PILs (Figure 2, systems 2-4 and 3-4). These systems are favorable for the EXAFS study as described below.

The copper(II) salts were generally much less soluble in the HHexam(Tf_2N)-PIL than in the HHexen(Tf_2N)-PIL, whereas $\text{Cu}(\text{Tf}_2\text{N})_2$ was somewhat soluble even in the HHexam(Tf_2N)-PIL (0.1 mol kg^{-1} ; Table 1), and the electronic spectrum of this latter solution was nearly identical with that of $\text{Cu}(\text{Tf}_2\text{N})_2$ in a concentrated $\text{HTf}_2\text{N}/\text{EtOH}$ solution (20.9 mol kg^{-1} ; Figure 1b). On the basis of the marked difference between the electronic spectra of $\text{Cu}(\text{hexen})_2(\text{Tf}_2\text{N})_2$ in ClF and $\text{Cu}(\text{Tf}_2\text{N})_2$ in the concentrated $\text{HTf}_2\text{N}/\text{EtOH}$ solution and because the spectrum of $\text{Cu}(\text{Tf}_2\text{N})_2$ in the HHexam(Tf_2N)-PIL is similar to that of $\text{Cu}(\text{Tf}_2\text{N})_2$ in the $\text{HTf}_2\text{N}/\text{EtOH}$ solution, it can be deduced that the copper(II) ion is predominantly surrounded by Tf_2N anions in the HHexam(Tf_2N)-PIL system.

EXAFS Study of the Interactions between Copper Ions and the PILs. EXAFS spectroscopic analysis of the Cu K-edge was used to directly monitor the interaction between the copper(II) ion and the PIL based on the nearest coordinating species around the copper(II) ion. Initially, the EXAFS spectra of bis-en and tris-en copper(II) complexes in the solid and usual solution states were acquired as typical species for which the coordination structures are established. Figure S3 in the SI shows the FT profiles (the x axis contains a phase shift) of the en complexes. In the case of some solid states (indicated by asterisks in Figure S3 in the SI), the coordination structures around the copper(II) ion have been elucidated in detail via X-ray crystallographic analysis. In the case of the solution system indicated by double circles, EXAFS studies have been reported, and the bond lengths determined herein are consistent with that of the previous report within error.¹⁴ The EXAFS FT profiles acquired for the bis-en and tris-en copper(II) complexes demonstrate that the intensities of the main FT profiles for the amine complex systems can be classified into two groups: the bis-en (or tetraammine) and tris-en systems, either in solid or in solution. Because the main peak will be assigned to the four equatorial nitrogen atoms due to the Jahn–Teller effect, the difference in the main-peak intensity can be attributed to the difference in the Debye–Waller parameters of the equatorial Cu–N bonds, as reported.²¹ On the basis of the electronic spectra, the coordination numbers (CNs) for the equatorial nitrogen atoms and for the axial nitrogen (or oxygen) atoms can be fixed as 4 and 2, respectively. Curve fitting of the FT profiles (Figure S3 in the SI) of the reference systems was performed, and the results are listed in Table S1 in the SI. The higher intensities of the FT peaks for the bis-en or tetraammine systems can be approximately attributed to the smaller Debye–Waller factors (σ) for the equatorial Cu–N bonds. This trend is reasonable because the $\text{Cu}^{\text{II}}\text{–N}$ moiety in the equatorial position of the bis-en complex has higher symmetry and may be more structurally rigid than that in the tris-en complex.²²

Thus, we hereafter discuss the EXAFS results for the Hexen complexation systems from two standpoints: first, by comparison of the FT profiles of the Hexen copper(II) complexes or of the copper(II) ion in the ionic liquid systems

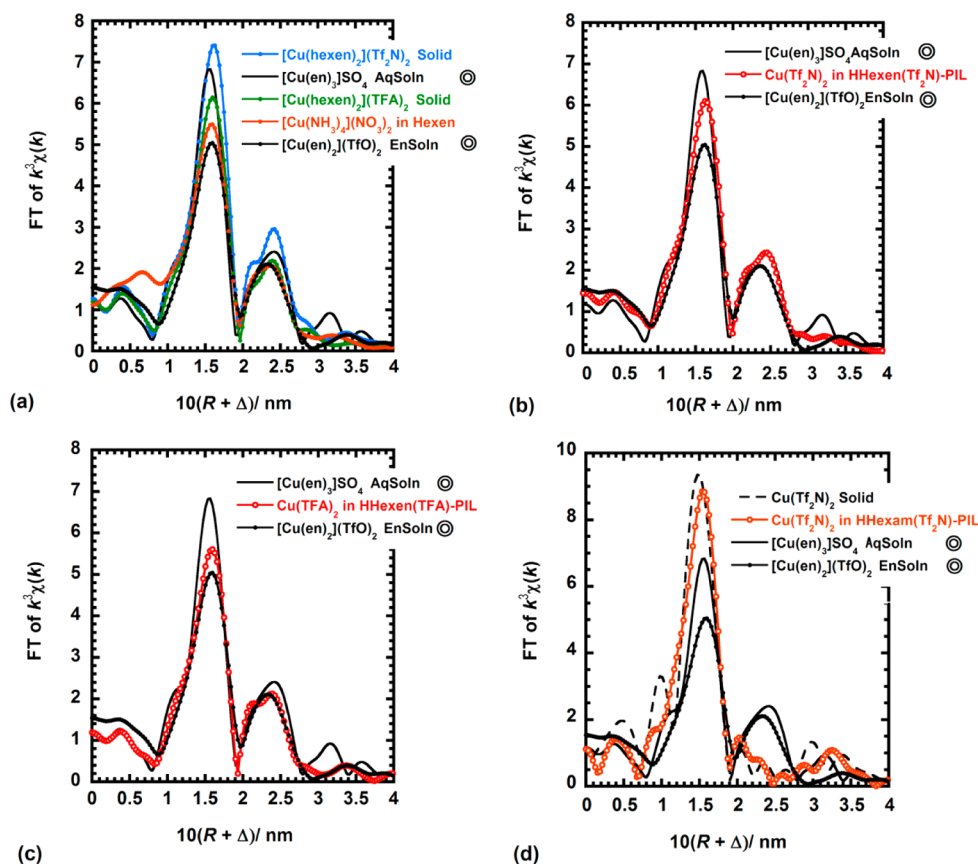


Figure 3. FTs $F(R)$ of the $k^3\chi(k)$ curves, uncorrected for phase shift. In all of the figures, the spectra marked with double circles in the legends are presented as those of archetypal references (a $[\text{Cu}(\text{en})_3]\text{SO}_4$ aqueous solution is the typical bis-en complex ($[\text{Cu}(\text{en})_2(\text{H}_2\text{O})_2]^{2+}$ in solution) and $[\text{Cu}(\text{en})_2](\text{TfO})_2$ in En solution is the typical tris-en complex ($[\text{Cu}(\text{en})_3]^{2+}$ in solution), as described in SI-2 and Figure S3 in the SI. In each figure, the system in focus is presented by a red line. Systems, other than the common references, are as follows: (a) Cu(hexen)₂X₂ (X = Tf₂N and TFA) complexes of solid states and $[\text{Cu}(\text{NH}_3)_4](\text{NO}_3)_2$ (0.03 mol kg⁻¹) in Hexen solution; (b) Cu(Tf₂N)₂ in HHexen(Tf₂N)-PIL (0.1 mol kg⁻¹); (c) Cu(TFA)₂ in HHexen(TFA)-PIL (0.1 mol kg⁻¹); (d) Cu(Tf₂N)₂ in solid and in HHexam(Tf₂N)-PIL (0.1 mol kg⁻¹).

with those of the well-established bis-en and tris-en complexes in solution (these two typical solution systems were selected and are indicated in Figure 3 by the double-circle mark) and, second, by determination of the EXAFS parameters by fixing the CNs to 4 (for the equatorial Cu–N) and 2 (for the axial Cu–N or Cu–O),¹⁴ as deduced from the visible electronic spectra.

Figure 3a shows the FT profiles of the Cu^{II}-hexen complexes in solution and in the solid state. It is notable that the hexen complexes show a characteristic peak ($2.0\text{--}2.7 \times 0.1$ nm on the x axis, where the phase shift is not corrected) arising from a weak second-shell contribution of the carbon in the coordinating en headgroup.^{14,23} The intensity of the main peak for $[\text{Cu}(\text{hexen})_2](\text{Tf}_2\text{N})_2$ in the solid state is comparable to that of the bis-en complex group, whereas the intensity of the peak for $[\text{Cu}(\text{hexen})_2](\text{TFA})_2$ in the solid state is intermediate between that of the bis-en and tris-en complex groups. The lower symmetry of the hexen ligand relative to the en ligand may account for the lower intensity of the peak of the $[\text{Cu}(\text{hexen})_2](\text{TFA})_2$ salt. The significantly higher intensity of the main peak for the Tf₂N salt may arise from the larger contribution of the Tf₂N anion in coordinating to the copper(II) ion to the intensity as described below. Figure 3a also shows the EXAFS FT profile of $[\text{Cu}(\text{NH}_3)_4](\text{NO}_3)_2$ in neat Hexen (0.03 mol kg⁻¹). The main peak of this system falls in the range of 0.1–0.2 nm, where the intensity is closer to that

of the tris-en reference system than to that of the bis-en system, which indicates that the major complex formed during complexation is the tris-hexen type in the Hexen system, which is consistent with the data from the visible electronic spectrum (Figure 2, system 1-2).

Parts b and c of Figure 3 show the FT spectra for the system containing 0.1 mol kg⁻¹ of Cu(A)₂ in the HHexen(A)-PIL (A = Tf₂N or TFA), along with the reference (double-circle marked) systems (the bis-en and tris-en complexes). On the basis of the aforementioned visible electronic spectral data, the solvation structure around the copper(II) ion remains largely unchanged from limiting dilution to a copper(II) concentration of 0.1 mol kg⁻¹ for the system comprising Cu(A)₂ in the HHexen(A)-PIL (Figure 2, systems 2-4 and 3-4). Therefore, the copper(II) EXAFS spectra of these systems are presented as exemplar spectra in Figure 3b,c. Very similar profiles were obtained when other copper(II) salts such as CuCl₂·2H₂O, CuBr₂, and $[\text{Cu}(\text{NH}_3)_4](\text{NO}_3)_2$ were used at a concentration of 0.1 mol kg⁻¹ in the respective HHexen(A)-PIL systems (data not presented), and the intensities of the main peaks in Figure 3b,c were 6.0 ± 0.5 and 5.5 ± 0.5 , respectively, for the various copper(II) salts used as additives; that is, the intensity of the main peak is essentially intermediate between those of the reference bis-en and tris-en groups. Although the bis-hexen copper(II) complexes are the species predominantly formed in the HHexen(Tf₂N)-PIL and HHexen(TFA)-PIL rather than

the tris-hexen complex, the greater structural fluctuation of these species in the PILs will give rise to a lower intensity of the main peak relative to the bis-en complex.

Figure 3d shows the FT spectrum of $\text{Cu}(\text{Tf}_2\text{N})_2$ in the HHexam(Tf_2N)-PIL along with that of solid $\text{Cu}(\text{Tf}_2\text{N})_2$; the profile is markedly different from that of the copper(II) ion in the chelating PILs and is more similar to the spectrum of solid $\text{Cu}(\text{Tf}_2\text{N})_2$. This result clearly indicates that the copper(II) ion is surrounded by the Tf_2N anion rather than the amines, which is consistent with the results of NMR (as described below) as well as the visible electronic spectra presented above (Figure 1b). Furthermore, the profile of the FT spectrum of $[\text{Cu}(\text{NH}_3)_4](\text{NO}_3)_2$ in the same PIL system (0.03 mol kg^{-1} ; data not presented) was very similar to that of $\text{Cu}(\text{Tf}_2\text{N})_2$ in Figure 3d. This indicates the high coordination strength of the Tf_2N anion to the copper(II) ion in this PIL system. Notably, the significantly higher peak intensity of the $\text{Cu}(\text{Tf}_2\text{N})_2$ solid relative to that of the en copper(II) complexes in Figure 3d is remarkable. X-ray crystallographic analyses have recently clarified that the four oxygen atoms of the $-(\text{SO}_2)_2$ moieties in $[\text{Cu}(\text{alkylimidazole})_2](\text{Tf}_2\text{N})_2$ are located close to the copper(II) ion.²⁴ That is, in the $\text{Cu}(\text{Tf}_2\text{N})_2$ solid, the nearest oxygen (eight in total) atoms may have a higher contribution to the first coordination peak of the copper(II) ion than the nearest (four) nitrogen atoms in the en and hexen complexes, and thus the peak intensity becomes significantly higher than that of the other complexes.^{21b}

Curve fitting was performed for complexation of the various Cu^{2+} -hexen systems (Figure S4 in the SI), where the CNs are fixed as 4 and 2 for the equatorial and axial sites, respectively; the results are listed in Table 3. The Cu^{2+} -N bond distances for the equatorial sites of monoalkyl-substituted En determined by X-ray crystallography are comparable at 0.200 nm for the primary amine and 0.204–0.208 nm for the secondary or tertiary amine.²⁵ The Cu^{2+} -N or Cu^{2+} -O bond distances of the axial sites in certain Cu^{2+} -en complexes are longer with values in the range of 0.220–0.260 nm. The σ values (Debye–Waller parameters) were estimated for the equatorial and axial sites as well. The σ values in the PILs are intermediate between those of the bis-en and tris-en complexes, but the differences are slight. It is not clear whether the lower intensity of the main peak relative to that of the bis-en complex group is derived from the larger fluctuation in the PILs or from the lower symmetry of the Hexen ligands.

Although the weak second peak of $R + \Delta = 0.2$ – 0.23 nm observed in the FT spectra of the complexes having an en chelate ring can be easily assigned to the Cu–C bond, a detailed discussion on the intensity and shape will be difficult owing to the indirect interaction and to the less experimental reliability compared to the main peak, as has been pointed out previously.^{14,23}

¹³C, ¹⁴N, and ¹⁵N NMR Spectroscopic Studies on the Interactions of Copper(II) Ions with the PILs and with the Hexen Molecular Liquid. The site-selective interactions of the Cu^{2+} ion in the PILs were monitored by determining the paramagnetic longitudinal relaxation times (T_{1p}) using ¹³C NMR and the paramagnetic line broadenings ($\Delta\nu_{1/2}$) of the ¹⁵N NMR spectra of the PILs. The HHexam(Tf_2N)-PIL and the molecular liquid of Hexen were mainly used in the NMR studies given that these two systems assume stable liquid states over a wide temperature range and are favorable for the temperature dependence study.

Table 3. Structural Parameters from EXAFS Analyses for the Copper(II) Ion of the Bis-hexen Complexes in the Solid State, in the HHexen-PILs, and in the neat Hexen

	bond	CN(fixed)	R (nm)	$10^3\sigma$ (nm)	r (%) ^a
I. Solid $\text{Cu}(\text{hexen})_2\text{X}_2$					
1. X = Tf_2N	Cu–N(eq)	4	0.202	7.6	
	Cu–C(eq)	4	0.283	7.8	4.5
	Cu–O(ax)	2	0.260	15.7	
2. X = TFA	Cu–N(eq)	4	0.202	8.5	
	Cu–C(eq)	4	0.282	8.4	4.5
	Cu–O(ax)	2	0.240	17.7	
II. In the PILs					
1. $\text{Cu}(\text{Tf}_2\text{N})_2$ in the HHexam(Tf_2N)-PIL	Cu–N(eq)	4	0.207	8.7	
	Cu–C(eq)	4	0.285	8.1	2.6
	Cu–O(ax)	2	0.230	20.0	
2. $\text{Cu}(\text{TFA})_2$ in the HHexam(TFA)-PIL	Cu–N(eq)	4	0.205	8.5	
	Cu–C(eq)	4	0.287	8.9	2.4
	Cu–O(ax)	2	0.220	15.7	
III. $[\text{Cu}(\text{NH}_3)_4](\text{NO}_3)_2$ in the Neat Hexen					
	Cu–N(eq)	4	0.206	9.5	
	Cu–C(eq)	4	0.288	9.3	2.3
	Cu–N(ax)	2	0.220	17.1	

^aThe r factor is defined as $\sum [k^3\chi(k)_{\text{obs}} - k^3\chi(k)_{\text{calc}}]^2 / \sum [k^3\chi(k)_{\text{obs}}]^2 \times 100$. The error bar of R was estimated by varying the ΔE value (± 10 eV) and the σ values (± 0.001 nm). The estimated error bars in the R values are ± 0.003 nm.

Parts a and b of Figure S5 in the SI respectively show the temperature dependence of the longitudinal relaxation times in the absence of copper(II) ions ($T_{1\text{dia}}$) for the neat Hexen and HHexam(Tf_2N)-PIL (see SI-3 in the SI). The slopes of the Arrhenius plots of $\log(T_{1\text{dia}})^{-1}$ versus T^{-1} were positive for the Hexen (above 15 °C) and PIL (above 30 °C) systems, and the τ_C values (correlation times) at 15 °C for the methylene moiety of the headgroup are significantly smaller than that of the boundary value. As a result, the extreme narrowing condition may largely hold in these systems, as described in SI-3 in the SI.²⁶

The paramagnetic relaxation rates (T_{1p}^{-1} and T_{2p}^{-1}), defined in the first part of eq 1, were obtained from ¹³C and ¹⁵N (or ¹⁴N) NMR, respectively. T_{ip}^{-1} for the nuclei in the headgroup of the Hexen unit can then be expressed by the modified Swift–Connick equation:^{14,27,28}

$$T_{ip}^{-1} = (T_{i\text{obs}})^{-1} - (T_{i\text{dia}})^{-1} = \frac{p_M q}{\tau_M + T_{iM}} \quad (i = 1 \text{ or } 2) \quad (1)$$

where $T_{i\text{obs}}$ is the relaxation time in the presence of the copper(II) salts, p_M is the molar ratio of copper(II) to the solvent under the condition where all of the copper(II) ions are

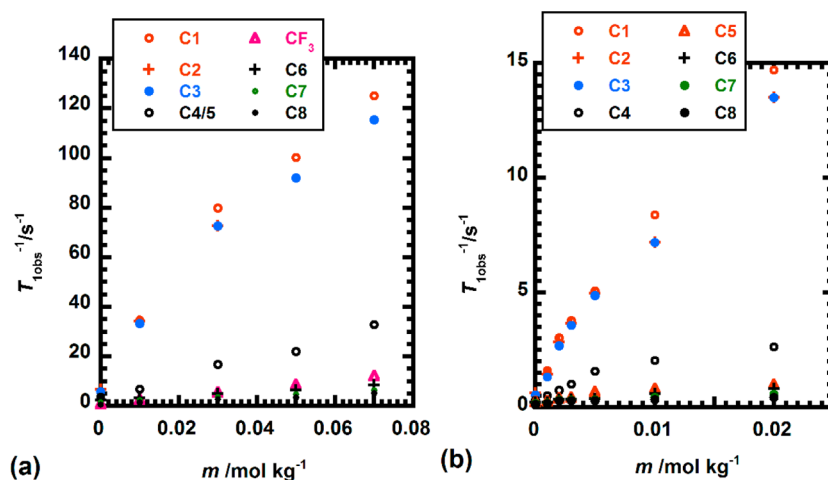


Figure 4. Dependence of ^{13}C $T_{1\text{obs}}$ on the $\text{Cu}(\text{Tf}_2\text{N})_2$ concentrations (m) for each carbon of (a) HHexen(Tf_2N)-PIL and (b) Hexen. The results for C2, C3, and C6–C8 are overlapped with each other.

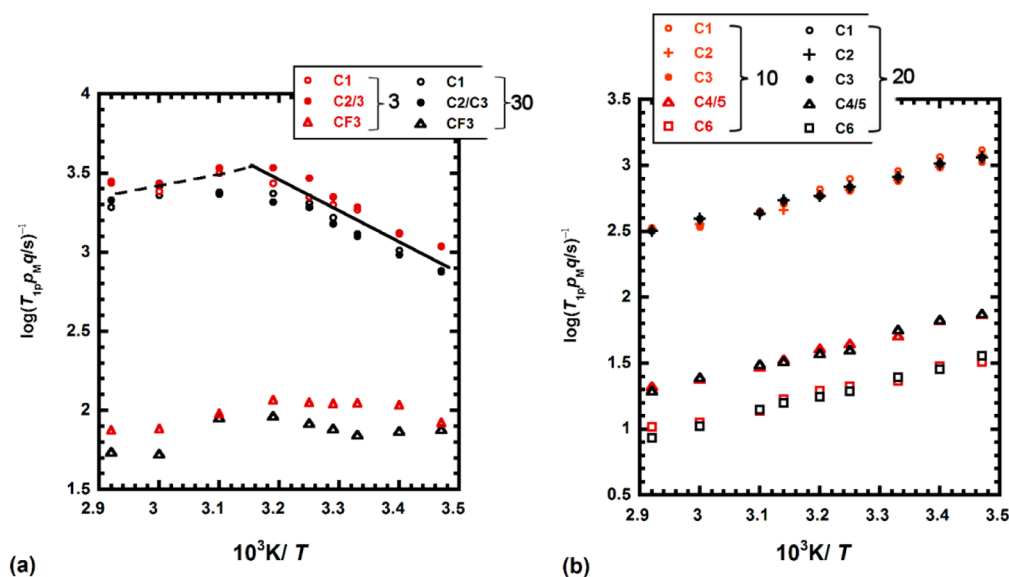


Figure 5. Temperature dependence of $\log(T_{1pMq})^{-1}$ for (a) the ^{13}C NMR of the carbons in the polar region of the HHexen(Tf_2N)-PIL in the presence of 3 mmol kg^{-1} (red) and 30 mmol kg^{-1} (black) $\text{Cu}(\text{Tf}_2\text{N})_2$ and (b) the Hexen in the presence of 10 mmol kg^{-1} (red) and 20 mmol kg^{-1} (black) $\text{Cu}(\text{Tf}_2\text{N})_2$.

bound to the solvent, q is the coordination number, τ_M is the residence of the Hexen ligand in the copper(II) complex, and T_{1M} is the relaxation time of the coordinated Hexen ligand.

According to the discussion presented in SI-3 in the SI, if the nucleus observed does not directly coordinate to the copper(II) ion (in all cases of the present ^{13}C NMR relaxations), the relaxation times will be mainly governed by the first term in eq S5 in the SI. On the other hand, if the nucleus observed directly coordinates to the copper(II) ion (in the major cases of the present ^{15}N NMR relaxations), T_{2M}^{-1} is mainly governed by the second term in eq S5 in the SI.

Thus, for the ^{13}C NMR relaxations, the present results (for Cu^{2+}) are interpreted on the basis of the equation^{27c,29}

$$T_{1M}^{-1} = \frac{2}{5} \left(\frac{\mu_0}{4\pi} \right)^2 \gamma_N^2 g_e^2 \mu_B^2 S(S+1) \frac{1}{r_{\text{CuC}}^6} \tau_C \quad (2)$$

where r_{CuC} is the distance between the metal center and the observed nucleus in the PIL, τ_C is the correlation time

described in SI-3 in the SI, and the other notations for the constants follow the conventional definition presented in SI-3 in the SI. On the other hand, for the copper(II)-bound nitrogen, the broadening of the ^{15}N line width [$\Delta\nu_{1/2} = (\pi T_{2p})^{-1}$] is correlated with T_{2M}^{-1} as follows:

$$T_{2M}^{-1} = \frac{2}{3} S(S+1) \left(\frac{A_C}{\hbar} \right)^2 \tau_S \quad (2')$$

where A_C is the hyperfine coupling constant and τ_S is the electronic relaxation time.

The assignments of the ^{13}C and ^{15}N NMR spectra of the present PILs have been reported in the previous paper,^{8c} and the paramagnetic relaxations of ^{13}C and ^{15}N NMR spectra can be interpreted herein from eqs 2 and 2', respectively, along with eq 1. Because the ^{13}C CF_3 peak was observed as a quartet, we took the larger two peaks and simply averaged the longitudinal relaxation times for the two peaks, which were almost the same.

In the ^{14}N NMR measurements, one broad signal was observed and is governed by the quadrupolar relaxation;

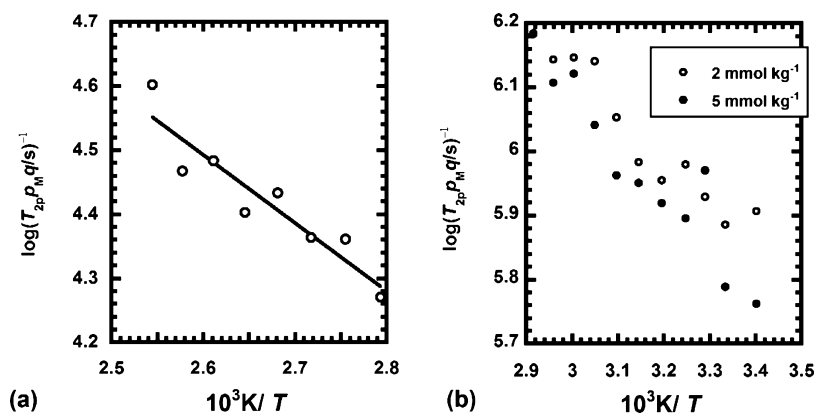


Figure 6. Temperature dependence of $\log(T_{2p}p_Mq)^{-1}$ for ^{14}N NMR of the nitrogen in the En moiety of (a) HHExen(Tf_2N)-PIL in the presence of 50 mmol kg^{-1} $\text{Cu}(\text{Tf}_2\text{N})_2$ and of (b) Hexen in the presence of 2 mmol kg^{-1} (○) and 5 mmol kg^{-1} (●) $\text{Cu}(\text{Tf}_2\text{N})_2$.

therefore, the result is used only for the estimation of τ_M on the basis of eq 1.

Comparison of HHExen(Tf_2N)-PIL System and the Hexen System. *Binding Sites of Cu^{2+} .* The T_{obs}^{-1} values determined from ^{13}C NMR for the HHExen(Tf_2N)-PIL and the Hexen molecular liquid in the presence of Cu^{2+} are plotted as a function of the copper(II) salt concentrations in parts a and b of Figure 4, respectively. The molar ratios (p_M) of the copper(II) salts to the solvent PIL and Hexen were $m/2.35$ and $m/6.93$, respectively. This plot corresponds to an increase in T_{1p}^{-1} with an increase in p_M as in eq 1. From eqs 1 and 2, it is understood that the stronger the interaction of Cu^{2+} with the moiety containing the ^{13}C nucleus, the larger the T_{1p}^{-1} value; thus, the interactions of Cu^{2+} with the C1, C2, and C3 carbons in the headgroup of the cationic unit are the strongest with comparable values.

Temperature Dependence of T_{1p} for ^{13}C NMR and T_{2p} for ^{14}N NMR in the HHExen(Tf_2N)-PIL and in the Hexen Molecular Liquid. Because both τ_M and τ_C in eqs 1 and 2, respectively, can be expressed by the Arrhenius-type relationship and T_{im}^{-1} is dominated by either the dipolar contribution (^{13}C NMR)^{27b} or the quadrupolar relaxation (^{14}N NMR),^{14,27e,28} the temperature dependence of T_{im}^{-1} ($i = 1$ or 2) and τ_M can be expressed as

$$T_{\text{im}}^{-1} = \frac{C_M}{T} \exp\left(\frac{E_M}{RT}\right) \quad (3)$$

$$\tau_M = \frac{h}{kT} \exp\left(\frac{\Delta G^\ddagger}{RT}\right) \quad (4)$$

where C_M is a constant independent of the temperature.

As presented in eqs 3 and 4, the temperature dependence of T_{im} and τ_M are inversely related, and thus we can decide which parameters of T_{im} and τ_M will govern T_{1p}^{-1} in eq 1 by monitoring the temperature dependence of T_{1p}^{-1} .^{14,27,28} For a direct comparison of the two systems, $\log(T_{1p}p_Mq)^{-1}$ is used on the ordinate of the plot, where $q = 4$ for the PIL system and 6 for the Hexen system based on the visible electronic spectral data and $p_M = m/2.35$ and $m/6.93$ in the PIL and in the neat Hexen, respectively. Parts a and b of Figure 5 present the $\log(T_{1p}p_Mq)^{-1}$ versus T^{-1} plot from ^{13}C NMR determination of T_{1p} in the HHExen(Tf_2N)-PIL (3 and 30 mmol kg^{-1}) and Hexen (10 and 20 mmol kg^{-1}) systems, respectively. A maximum is observed in Figure 5a, i.e., at higher temperature, T_{1M} may be dominant, whereas at lower temperature, τ_M may

be dominant.^{14,28} From Figure 5a, the τ_M value at 44°C (maximum point) in the HHExen(Tf_2N)-PIL system can be roughly estimated to be around $10^{-3.6}$ s. In the Hexen system (Figure 5b), the slope is consistently positive and thus T_{1M} will always govern T_{1p} . When T_{1p} was measured at two concentrations in the PIL system (Figure 5a), the agreement of the $\log(T_{1p}p_Mq)$ values between the two concentrations (3 and 30 mmol kg^{-1}) was better for the polar-group carbons than for the alkyl-chain carbons, and thus Figure 5a presents the results only for the polar groups. Although eq 2 for the relaxation times T_{1M} includes some assumptions, we can, in principle, estimate the relative locations of the carbon atoms (r_{CuC}) in the copper(II) complex in eq 2 by comparing the different moieties of the carbons in the molecule (Figure 5). For this purpose, the longitudinal relaxation times of the C1 and CF_3 carbons at 70°C ($10^3 \text{ K}/T = 2.92$, in Figure 5a) in the HHExen(Tf_2N) system are used as the moieties of the respective cationic and anionic units because the T_1 values of all of the systems may be governed by the D–D interactions at 70°C (τ_M can be neglected in eq 1) and the ^{13}C NMR spectra of C1 and CF_3 were most clearly and independently obtained.

The $\tau_C(\text{C1})$ and $\tau_C(\text{CF}_3)$ values can be assumed to be identical in the core part of the copper(II) complex of the HHExen(Tf_2N)-PIL system, and thus $\log[T_{1p}p_Mq(\text{C1})/T_{1p}p_Mq(\text{CF}_3)]^{-1}$ is proportional to $\log[r_{\text{CuC}}(\text{C1})/r_{\text{CuC}}(\text{CF}_3)]^{-6}$ based on eqs 1 and 2. When we use the relaxation times at 70°C , $\log[T_{1p}p_Mq(\text{C1})/T_{1p}p_Mq(\text{CF}_3)]^{-1}$ is ca. 1.55 and therefore the $r_{\text{CuC}}(\text{CF}_3)/r_{\text{CuC}}(\text{C1})$ ratio is estimated to be 1.8. According to the result of EXAFS listed in Table 3, the $r_{\text{CuO}}[\text{Tf}_2\text{N}(\text{ax})]/r_{\text{CuC}}[\text{C1}(\text{eq})]$ ratio of 0.81 and thus the CF_3 moiety in the Tf_2N anion may be located outside the core of the copper(II) complex. The two CF_3 moieties in Tf_2N may become different in the copper(II) complex, but they cannot be discriminated in the NMR measurement, and thus the information obtained here is the time-averaged location for the two kinds of CF_3 .

In the Hexen liquid system, on the other hand, the C1 and C6 carbons are selected for comparison to estimate the relative intramolecular locations in the copper(II) complex using the results of the relaxation times at 70°C in Figures 5b and S5b in the SI. In this system, because both the C1 and C6 carbons are the moiety of the methylene group, we can use eq S2 in the SI in common and the result of Figure S5b in the SI. If the $\tau_C(\text{C1})/\tau_C(\text{C6})$ ratio is assumed to be the same in the absence (Figure S5b in the SI) and presence (Figure 6b) of Cu^{2+} , the value of $\log[T_{1p}p_Mq(\text{C1})/T_{1p}p_Mq(\text{C6})]^{-1} - \log[T_{1\text{dia}}(\text{C1})/$

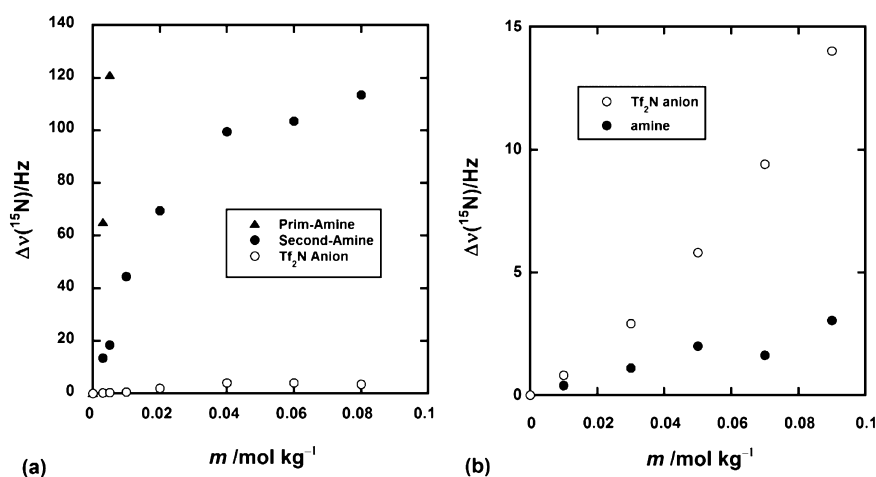


Figure 7. Dependence of ^{15}N NMR line broadenings $[\Delta\nu(^{15}\text{N})]$ on the $\text{Cu}(\text{Tf}_2\text{N})_2$ concentrations for each carbon in (a) the HHexen(Tf_2N)-PIL and (b) the HHexam(Tf_2N)-PIL.

$T_{\text{dia}}(\text{C6})^{-1}$ is ca. 1.50, and thus $r_{\text{CuC}}(\text{C6})/r_{\text{CuC}}(\text{C1})$ is estimated to be 1.8. Because $r_{\text{CuC}}(\text{C6})/r_{\text{CuC}}(\text{C1})$ in the Hexen and $r_{\text{CuC}}(\text{CF}_3)/r_{\text{CuC}}(\text{C1})$ in the PIL are identical, similar locations of the CF_3 moiety in the copper(II) complex of the HHexen(Tf_2N)-PIL and of the C6 moiety in the copper(II) complex of Hexen relative to the en headgroup are presumed.

When eq 1 is applied to the determination of T_{2p}^{-1} from ^{14}N NMR,^{14,28} the contribution of T_{2M} to the denominator of eq 1 should be smaller because of quadrupolar relaxation than that of T_{1M} in the ^{13}C NMR relaxation; i.e., τ_M predominates T_{2M} in eq 1. Thus, the τ_M values for both the HHexen(Tf_2N)-PIL and Hexen systems can be determined directly from the temperature dependence of T_{2p}^{-1} from ^{14}N NMR.

Because the ^{14}N NMR signal could be clearly detected only at higher temperature in the PIL system, the temperature dependence was monitored in the range of 85–120 °C for the PIL system ($[\text{Cu}(\text{Tf}_2\text{N})_2] = 50 \text{ mmol kg}^{-1}$), whereas for the neat Hexen system, the evaluated range was 20–70 °C ($[\text{Cu}(\text{Tf}_2\text{N})_2] = 2$ and 5 mmol kg^{-1}). The Arrhenius plots of $\log(T_{2p}p_Mq)^{-1}$ versus T^{-1} for the ^{14}N NMR line widths are presented in parts a and b of Figure 6 for the PIL and neat Hexen systems, respectively. The data are somewhat scattered, but these plots clearly have negative slopes for both the PIL and Hexen systems. Thus, it can be deduced that T_{2p}^{-1} should be governed by τ_M . On the basis of this result, the τ_M values were estimated to be $(2.5\text{--}5.3) \times 10^{-5} \text{ s}$ (120–85 °C) for the PIL, where the CN (q) for the Cu^{2+} -hexen complex is taken as 4. By taking into account the difference in the observed temperature, we can consider that these values are of the same order of magnitude as $\tau_M = 2.5 \times 10^{-4} \text{ s}$ at 44 °C, estimated from the ^{13}C NMR relaxations (Figure 5a). Furthermore, the ΔH^\ddagger value ($\Delta G^\ddagger = \Delta H^\ddagger - T\Delta S^\ddagger$ in eq 4) is estimated to be 19 kJ mol^{-1} from the slope. The τ_M value obtained from ^{14}N NMR may be more reliable than that from ^{13}C NMR because the former methodology directly monitors the complexation of copper(II) to the en headgroup. It can be concluded that in the PIL the τ_M value is on the order of 10^{-4} s at ambient temperature.

In the neat Hexen system, the τ_M value could only be obtained from the ^{14}N NMR line widths. The $\log(T_{2p}p_Mq)^{-1}$ versus T^{-1} plot for the Hexen in the presence of $\text{Cu}(\text{Tf}_2\text{N})_2$ ($[\text{Cu}(\text{Tf}_2\text{N})_2] = 2$ and 5 mmol kg^{-1}), where q is taken as 6, is shown in Figure 6b. The τ_M value is in the range of 6.3×10^{-7} – $1.6 \times 10^{-6} \text{ s}$ (70–20 °C) in the neat Hexen.

It is interesting to compare the lifetimes of Cu^{2+} in various solvents; i.e., at room temperature, they follow the order HHexen(Tf_2N)-PIL (10^{-4} s) \gg neat Hexen (10^{-6} s) $>$ neat En (10^{-7} s)¹⁴ $>$ EtOH ($1.4 \times 10^{-8} \text{ s}$)¹⁴ $>$ water ($2 \times 10^{-9} \text{ s}$).¹⁴ The much longer lifetimes of Cu^{2+} in the present PIL and the significantly longer lifetimes in the neat Hexen reflect the extent of the confinement of the copper(II) ion in these organized solutions.

^{15}N NMR Line Broadenings for the HHexen(Tf_2N)-PIL and HHexam(Tf_2N)-PIL Systems. In comparison with the ^{13}C NMR spectrum, the ^{15}N NMR spectrum of the primary amine was significantly broader than that of the secondary amine as shown in Figure 7(a) in which the $\text{Cu}(\text{Tf}_2\text{N})_2$ concentration was varied. This difference can be explained based on the difference in the contact term (eq 2') of the primary and secondary amines, as discussed in SI-3 in the SI.³⁰ The small broadening of the ^{15}N NMR $[\Delta\nu(^{15}\text{N})]$ peaks in the case of the Tf_2N anion (below 5 Hz in Figure 7a) indicates less interaction of the nitrogen atom in this anion with the copper(II) ion.

In the case of the monoamine HHexam(Tf_2N)-PIL (Figure 7b), the broadening of the ^{15}N NMR spectra $[\Delta\nu(^{15}\text{N})]$ of the amine in the cationic unit was much smaller (3 Hz) than that of the HHexen(Tf_2N) system in the presence of $\text{Cu}(\text{Tf}_2\text{N})_2$ (0.09 mol kg^{-1}), whereas the ^{15}N NMR for the anionic unit was significantly broader (15 Hz) than that in the HHexen(Tf_2N) system (3 Hz), as shown in Figure 7b. However, the extent of the broadening for the Tf_2N anion was much smaller than that observed for the En unit of the HHexen(A)-PIL, where the copper(II) ion binds directly to the nitrogen atoms. Thus, in the case of the HHexam(Tf_2N)-PIL, the broadening of the ^{15}N NMR spectra due to Cu^{2+} can be largely attributed to dipolar relaxation, and the interaction of the copper(II) ion with the PIL is mainly governed by the electrostatic force, whereas the nitrogen atom of the Tf_2N anion should not bind directly to the copper(II) ion.

CONCLUSIONS

A coordination mode of the copper(II) ion in the ionic liquids having chelate amine was studied using NMR, visible electronic spectra, and EXAFS. In spite of the electrostatic repulsion, the copper(II) ion is preferentially coordinated by the cationic unit in the HHexen(Tf_2N) to release the proton from the PIL,

whereas in the hexylammonium-Tf₂N, the copper(II) ion prefers the anionic unit. The copper(II) ion dominantly interacts with the two en headgroups (formation of the bis-hexen complex) in the cationic unit of the HHexen-PIL. The axial coordination sites are occupied by the Tf₂N or TFA anion at lower Cu²⁺ concentrations; in the Tf₂N-PIL system, with an increase in the Cu²⁺ concentrations, the axial Tf₂N anion is gradually replaced by the ligands of the added copper(II) salts, whereas the TFA anions in the axial coordination sites are almost kept binding to the copper(II) ion. By using both the ¹³C NMR longitudinal relaxations and ¹⁴N NMR line widths, the lifetime of the copper(II) complex formed in the HHexen(Tf₂N)-PIL was determined to be around 10⁻⁴ s, which is significantly longer than that (10⁻⁶ s order) in the molecular solvent of Hexen. The author emphasizes the suitability of the paramagnetic NMR relaxation study on solvation of the metal ion to the present ionic liquid system compared to the conventional molecular liquid systems from the viewpoint of the time scale.

■ ASSOCIATED CONTENT

■ Supporting Information

Visible absorption spectra (Figure S1) and EXAFS data (Figure S3 and Table S1) of the copper(II) ethylenediamine complexes, preparations and characterizations of the PILs and copper(II) complexes (SI-1 and SI-2), approximation for the NMR relaxations (SI-3), temperature dependence of the longitudinal relaxation times for the HHexen(Tf₂N)-PIL and for the neat Hexen in the absence of the copper(II) ion (Figure S5), EXFAS data for the Hexen systems (Figure S4), and the λ_{\max} change with the addition of bromide ion to [Cu(Hexen)₂]²⁺ in CLF (Figure S2). This material is available free of charge via the Internet at <http://pubs.acs.org>.

■ AUTHOR INFORMATION

Corresponding Author

*E-mail: iida@cc.nara-wu.ac.jp. Fax: +81742203397.

Notes

The authors declare no competing financial interest.

■ ACKNOWLEDGMENTS

This work was financially supported by a Nara Women's University Intramural Grant for Project Research and by a Grant-in-Aid for Scientific Research (Grant 25410191). The X-ray absorption spectral study was performed with the approval of the Photon Factory Advisory Committee (Proposal Nos. 2011G510 and 2013G009). Thanks are due to the Instrument Center in the Institute for Molecular Science for assistance in the NMR (JNM Lambda 500) measurements. We are grateful to Dr. Tsukasa Imanari at Chiba University for helpful discussion in the NMR studies and to Kazufumi Chifuku at the Division of Instrumental Analysis of Nagasaki University for measurements of elemental analyses.

■ REFERENCES

- (1) (a) Canongia Lopes, J. N.; Pádua, A. A. H. *J. Phys. Chem. B* **2006**, *110*, 3330–3335. (b) Rebelo, L. P. N.; Canongia Lopes, J. N.; Esperança, J. M. S. S.; Guedes, H. J. R.; Lachwa, J.; Visak, V.-N.; Visak, Z. P. *Acc. Chem. Res.* **2007**, *40*, 1114–1121. (c) Triolo, A.; Russina, O.; Bleif, H.-J.; Cola, E. D. *J. Phys. Chem. B* **2007**, *111*, 4641–4644.
- (2) (a) Huang, J.-F.; Luo, H.; Dai, S. *J. Electrochem. Soc.* **2006**, *153*, 9–13. (b) Taubert, A.; Li, Z. *Dalton Trans.* **2007**, 723–727. (c) Scheeren, C. W.; Domingos, J. B.; Machado, G.; Dupont, J. J. *Phys. Chem. C* **2008**, *112*, 16463–16469. (d) Iida, M.; Baba, C.; Inoue,

- M.; Yoshida, H.; Taguchi, E.; Furusho, H. *Chem.—Eur. J.* **2008**, *14*, 5047–5056. (e) Dupont, J.; Scholten, J. D. *Chem. Soc. Rev.* **2010**, *39*, 1780–1804. (f) Ma, Z.; Yu, J.; Dai, S. *Adv. Mater.* **2010**, *22*, 261–285. (g) Luska, K. L.; Moores, A. *ChemCatChem* **2012**, *4*, 1534–1546. (h) Kaur, R.; Mehta, S. K. *Coord. Chem. Rev.* **2014**, *262*, 37–54.
- (3) (a) Gao, Y.; Twamley, B.; Shreeve, J. M. *Inorg. Chem.* **2004**, *43*, 3406–3412. (b) Lin, I. J. B.; Vasam, C. S. *J. Organomet. Chem.* **2005**, *690*, 3498–3512. (c) Binnemans, K. *Chem. Rev.* **2007**, *107*, 2592–2614. (d) Taubert, A. *Top. Curr. Chem.* **2009**, *290*, 127–159. (e) Anderson, T. M.; Ingersoll, D.; Rose, A. J.; Staiger, C. L.; Leonard, J. C. *Dalton Trans.* **2010**, 39, 8609–8612. (f) Miura, Y.; Shimizu, F.; Mochida, T. *Inorg. Chem.* **2010**, *49*, 10032–10040. (g) Pratt, H. D., III; Rose, A. J.; Staiger, C. L.; Ingersoll, D.; Anderson, T. M. *Dalton Trans.* **2010**, *40*, 11396–11401. (h) Brooks, N. R.; Schaltin, S.; Van Hecke, K.; Van Meervelt, L.; Binnemans, K.; Fransaer, J. *Chem.—Eur. J.* **2011**, *17*, 5054–5059. (i) Inagaki, T.; Mochida, T.; Takahashi, M.; Kanadani, C.; Saito, T.; Kuwahara, D. *Chem.—Eur. J.* **2012**, *18*, 6795–6804. (j) Funasako, Y.; Mochida, T.; Takahashi, K.; Sakurai, T.; Ohta, H. *Chem.—Eur. J.* **2012**, *18*, 11929–11936. (k) Mochida, T.; Funasako, Y.; Inagaki, T.; Li, M.-J.; Asahara, K.; Kuwahara, D. *Chem.—Eur. J.* **2013**, *19*, 6257–6264. (l) Schaltin, S.; Brooks, N. R.; Sniekers, J.; Depuydt, D.; Merrvelt, L. V.; Binnemans, K.; Fransaer, J. *Phys. Chem. Chem. Phys.* **2013**, *15*, 18934–18943. (m) Sniekers, J.; Brooks, N. R.; Schaltin, S.; Merrvelt, L. V.; Fransaer, J.; Binnemans, K. *Dalton Trans.* **2014**, 43, 1589–1598.
- (4) (a) Visser, A. E.; Swatoski, R. P.; Reichert, W. M.; Mayton, R.; Sheff, S.; Wierzbicki, A.; Davis, J. H., Jr.; Rogers, R. D. *Chem. Commun.* **2001**, 135–136. (b) Davis, J. H., Jr. *Chem. Lett.* **2004**, 33, 1072–1075. (c) Nockemann, P.; Thijs, B.; Pittois, S.; Thoen, J.; Glorieux, C.; Van Hecke, K.; Van Meervelt, L.; Kirchner, B.; Binnemans, K. *J. Phys. Chem. B* **2006**, *110*, 20978–20992. (d) Nockemann, P.; Thijs, B.; Parac-Vogt, T. N.; Van Hecke, K.; Van Meervelt, L.; Tinant, B.; Hartenbach, I.; Sclid, T.; Ngan, V. T.; Nguyen, M. T.; Binnemans, K. *Inorg. Chem.* **2008**, *47*, 9987–9999. (e) Reyna-González, J. M.; Torriero, A. A. J.; Siriwardana, A. I.; Burgar, I. M.; Bond, A. M. *Anal. Chem.* **2010**, *82*, 7691–7698.
- (5) (a) Hardacre, C.; Holbrey, J. D.; Nieuwenhuysen, M.; Youngs, T. G. *Acc. Chem. Res.* **2007**, *40*, 1146–1155. (b) Abbott, A. P.; Frisch, G.; Ryder, K. S. *Annu. Rep. Prog. Chem., Sect. A* **2008**, *104*, 21–45. (c) Fujii, K.; Nonaka, T.; Akimoto, Y.; Umebayashi, U.; Ishiguro, S. *Anal. Sci.* **2008**, *24*, 1377–1380. (d) Nockemann, P.; Thijs, B.; Lunstroot, K.; Parac-Vogt, T. N.; Görrler-Walrand, C.; Binnemans, K.; Van Hecke, K.; Van Meervelt, L.; Nikitenko, S.; Daniels, J.; Hennig, C.; Van Deun, R. *Chem.—Eur. J.* **2009**, *15*, 1449–1461. (e) Li, G.; Camaioni, D. M.; Amonette, J. E.; Zhang, Z. C.; Johnson, T. J.; Fulton, J. L. *J. Phys. Chem. B* **2010**, *114*, 12614–12622.
- (6) (a) Er, H.; Asaoka, N.; Hisamatsu, N.; Iida, M.; Imae, T. *Colloids Surf., A* **2003**, *221*, 119–129. (b) Iida, M.; Inoue, M.; Tanase, T.; Takeuchi, T.; Sugibayashi, M.; Ohta, K. *Eur. J. Inorg. Chem.* **2004**, 3920–3929. (c) Er, H.; Ohkawa, S.; Iida, M. *Colloids Surf., A* **2007**, *301*, 189–198.
- (7) (a) Greaves, T. L.; Weerawardena, A.; Fong, C.; Krodskiewska, I.; Drummond, C. J. *J. Phys. Chem. B* **2006**, *110*, 22479–22487. (b) Angell, C. A.; Byrne, C. A. N.; Belieres, J.-P. *Acc. Chem. Res.* **2007**, *40*, 1228–1236. (c) Nuthakki, B.; Greaves, T. L.; Krodskiewska, I.; Weerawardena, A.; Burgar, M. I.; Mulder, R. I.; Drummond, C. J. *Aust. J. Chem.* **2007**, *60*, 21–28. (d) Belieres, J.-P.; Angell, C. A. *J. Phys. Chem. B* **2007**, *111*, 4926–4937. (e) Greaves, T. L.; Drummond, C. J. *Chem. Rev.* **2008**, *108*, 206–237. (f) Angell, C. A.; Ansari, Y.; Zhao, Z. *Faraday Discuss.* **2012**, *154*, 9–27. (g) Ueno, K.; Yoshida, K.; Tsuchiya, M.; Tachikawa, N.; Dokko, K.; Watanabe, M. *J. Phys. Chem. B* **2012**, *116*, 11323–11331.
- (8) (a) Iida, M.; Syouno, E.; Kawakami, S.; Hanai, M. *Chem. Lett.* **2009**, *38*, 544–545. (b) Iida, M.; Kawakami, S.; Syouno, E.; Er, H.; Taguchi, E. *J. Colloid Interface Sci.* **2011**, *356*, 630–638. (c) Watanabe, M.; Takemura, S.; Kawakami, S.; Syouno, E.; Kurosu, H.; Harada, M.; Iida, M. *J. Mol. Liq.* **2013**, *183*, 50–58.
- (9) (a) De Vreese, P.; Brooks, N. R.; Van Hecke, K.; Van Merrvelt, L.; Matthijs, E.; Binnemans, K.; Van Deun, R. *Inorg. Chem.* **2012**, *51*,

4972–4981. (b) Caporali, S.; Chiappe, C.; Ghilardi, T.; Pomelli, C. S.; Pinzino, C. *ChemPhysChem* **2012**, *13*, 1885–1892. (c) Takao, K.; Tone, Y.; Hennig, C.; Inoue, S.; Tsubomura, T. *Inorg. Chem.* **2012**, *51*, 4850–4854. (d) Pokorny, K.; Schmeisser, M.; Hampel, F.; Zahl, A.; Puchta, R.; van Eldik, R. *Inorg. Chem.* **2013**, *52*, 13167–13178.

(10) Bruno, A. J.; Chaberek, S.; Martell, A. E. *J. Am. Chem. Soc.* **1956**, *78*, 2723–2728.

(11) Iida, M.; Asayama, K.; Ohkawa, S. *Bull. Chem. Soc. Jpn.* **2002**, *75*, 521–529.

(12) Naren, G.; Yasuda, A.; Iida, M.; Harada, M.; Suzuki, T.; Kato, M. *Dalton Trans.* **2009**, 5512–5522.

(13) (a) Morosin, B. *Acta Crystallogr.* **1976**, *B32*, 1237–1240. (b) Cola, M.; Giuseppetti, G.; Mazzi, F. *Atti Sci. Cl. Sci. Fis.* **1962**, *96*, 381–408. (c) Bertini, I.; Dapporto, P.; Gatteschin, D.; Scozzafava, A. *J. Chem. Soc., Dalton Trans.* **1979**, 1409–1414.

(14) Inada, Y.; Ozutsumi, K.; Funahashi, S.; Soyama, S.; Kawashima, T.; Tanaka, M. *Inorg. Chem.* **1993**, *32*, 3010–3014.

(15) McKale, A. G.; Veal, B. W.; Paulikas, A. P.; Chan, S. K.; Knapp, G. S. *J. Am. Chem. Soc.* **1988**, *110*, 3763–3768.

(16) Complexations of Cu^{2+} with the long-chained alkylethylenediamines in dilute aqueous solutions have been previously studied. (a) Lu, X.; Zhang, Z.; Liang, Y. *Langmuir* **1996**, *12*, 5501–5503. (b) Lu, X.; Zhang, Z.; Liang, Y. *Langmuir* **1997**, *13*, 533–538. (c) Li, C.; Lu, X.; Liang, Y. *Langmuir* **2002**, *18*, 575–580.

(17) Martell, A.; Sillén, L. G. *Stability Constants of Metal-Ion Complexes*; The Chemical Society: London, 1964; pp 371–373.

(18) (a) Fukuda, Y.; Sone, K. *Bull. Chem. Soc. Jpn.* **1972**, *45*, 465–469. (b) Fukuda, Y.; Yasuhira, M.; Sone, K. *Bull. Chem. Soc. Jpn.* **1985**, *58*, 3518–3523. (c) Muldoon, M. J.; Gordon, C. M.; Dunkin, I. R. *J. Chem. Soc., Perkin Trans. 2* **2001**, 433–435.

(19) (a) Holzweber, M.; Lungwitz, R.; Doerfler, D.; Spange, S.; Koel, M.; Hutter, H.; Linert, W. *Chem.—Eur. J.* **2013**, *19*, 288–293. (b) Gutman, V. *The Donor–Acceptor Approach to Molecular Interactions*; Springer: Berlin, Germany, 1978; Chapter 2.

(20) The value for Te_2N^- was estimated from ref 19.

(21) (a) Miyanaga, T.; Sakane, H.; Watanabe, I. *Bull. Chem. Soc. Jpn.* **1995**, *68*, 819–824. (b) Hardacre, C. *Annu. Rev. Mater. Res.* **2005**, *35*, 29–49.

(22) For example, see: Hill, H. A. O.; Day, P. *Physical Methods in Advanced Inorganic Chemistry*; John Wiley and Sons: London, 1968; Chapter 4, pp 109–111.

(23) Carriat, J. Y.; Che, M.; Kermarec, M.; Verdaguer, M.; Michalowicz, A. *J. Am. Chem. Soc.* **1998**, *120*, 2059–2070.

(24) Hoogerstraete, T. V.; Brooks, N. R.; Norberg, B.; Wouters, J.; Hecke, K. V.; Meervelt, L. V.; Binnemans, K. *CrystEngComm* **2012**, *14*, 4902–4911.

(25) (a) Walsh, A.; Hathaway, B. J. *J. Chem. Soc., Dalton Trans.* **1984**, 15–18. (b) Kansikas, J. *Acta Chem. Scand. A* **1987**, *A41*, 533–538. (c) Akitsu, T.; Einaga, Y. *Inorg. Chim. Acta* **2007**, *360*, 497–505.

(26) (a) Antony, J. H.; Mertens, D.; Dölle, A.; Wasserscheid, P.; Carper, W. R. *ChemPhysChem* **2003**, *4*, 588–594. (b) Imanari, M.; Uchida, K.; Miyano, K.; Seki, H.; Nishikawa, K. *Phys. Chem. Chem. Phys.* **2010**, *12*, 2959–2967. (c) Amamikov, V. P. *Chem. Rev.* **2011**, *111*, 418–454.

(27) (a) Swift, J. T. In *NMR of Paramagnetic Molecules*; La Mar, G. N., Horrocks, W. D., Holm, R. H., Jr.; Academic Press: New York, 1973; Chapter 2, pp 53–83. (b) Kitagawa, S.; Yoshikawa, K.; Morishima, I. *J. Phys. Chem.* **1978**, *82*, 89–97. (c) Chachaty, C. *Prog. NMR Spectrosc.* **1987**, *19*, 183–222. (d) Evans, J. N. S. *Biomolecular NMR Spectroscopy*; Oxford University Press: Oxford, U.K., 1995; Chapter 3, pp 127–129, and Chapter 7, pp 282–288. (e) Bertini, I.; Luchinat, C. *Coord. Chem. Rev.* **1996**, *150*, 77–130.

(28) Funahashi, S.; Nishimoto, T.; Hioki, A.; Tanaka, M. *Inorg. Chem.* **1981**, *20*, 2648–2651.

(29) Shulman, R. G.; Sternlicht, H.; Wyluda, B. *J. Chem. Phys.* **1965**, *43*, 3116–3122.

(30) Yokoi, H.; Isobe, T. *Bull. Chem. Soc. Jpn.* **1969**, *42*, 2187–2193.